Great Lakes Radar Technical Report

Spring 2018 Season on Lake Superior

U.S. Fish and Wildlife Service, Region 3

Funding Provided by Great Lakes Restoration Initiative

2019

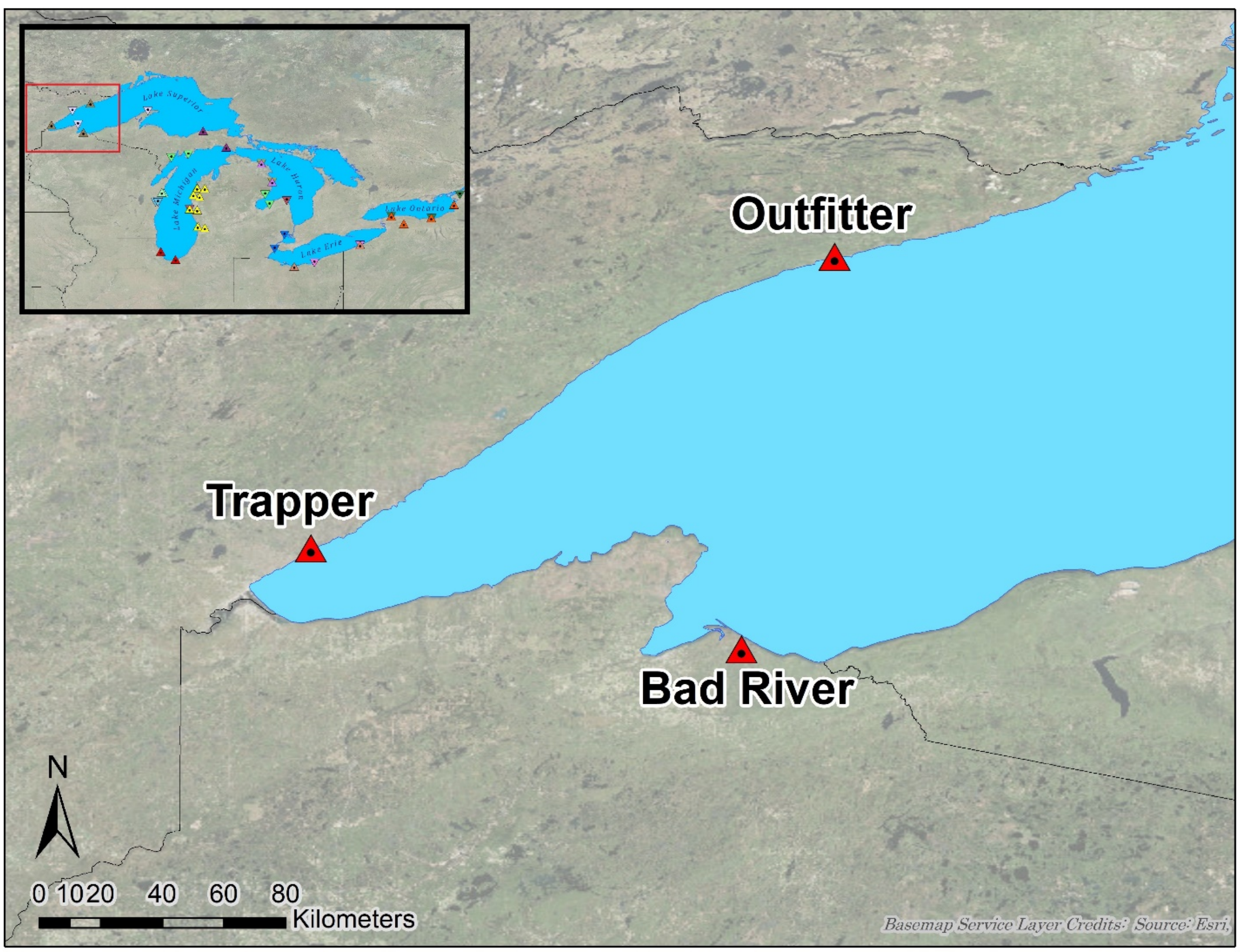

Recommended citation:

Rathbun, N.A., Heist, K.W., Wells, M.T., and Rigby, E.A. 2019. Great Lakes Radar Technical Report Lake Superior, Spring 2018. U.S. Department of Interior, Fish and Wildlife Service.

Table of Contents

Tables and Figures

INTRODUCTION

Global wind patterns help to move millions of migrating birds and bats through the Great Lakes region where shorelines provide important stopover habitat. Shorelines are thought to concentrate migrants as they offer the last refuge near a geographic obstacle and are likely used by migrants for navigation. Shorelines also may be subject to human development, including buildings, towers, and wind energy infrastructure. These structures may be detrimental to migrating birds and bats, potentially causing avoidance, injury, or mortality due to collisions. Although migration flyways are broadly understood, site-specific information about migration in the Great Lakes is lacking. Many migrants travel nocturnally, making observations difficult. Site-specific information about migration in the Great Lakes region would assist decision-makers in siting infrastructure to avoid and minimize negative impacts to migrating birds and bats.

To provide information about bird and bat migration in the Great Lakes region to developers, agencies, and other stakeholders, the U.S. Fish and Wildlife Service investigated the aeroecology of the Great Lakes shorelines. We used avian radar systems to identify activity patterns, timing, and duration of migration that occurred along shorelines of the Great Lakes. This report contains information from a study conducted by the U.S. Fish and Wildlife Service Avian Radar Team during the spring of 2018. The report is intended to provide data on the use of airspace around the western side of Lake Superior by aerial migrant birds and bats.

METHODS

An abbreviated description of methods relevant to the figures and data provided in this report is included here. A more thorough methodology can be found in Rathbun *et al*. 2016.

<u>Study Area</u>

During the spring 2018 season, we deployed radar units at three different sites (Table 1). We selected one site on the south shore of Lake Superior within the Bad River Band of the Lake Superior Tribe of Chippewa Indians Reservation, WI (Bad River) in order to study the behavior of migrants approaching Lake Superior from the south. We selected two other sites on the north shore of Lake Superior to study migrant lake crossing and coastal use in this area, and moved the radar unit between them during the season. One site was northeast of Duluth, MN (Trapper Site). The second was southwest of Grand Marais, MN (Outfitter Site).

Site	Nearby Town	Latitude	Longitude	Distance to Lake Shore (km)	Start Date	End Date
Bad River	Odanah, WI	46.602390° N	-90.656160° W	3.25	4/5/18	6/27/18
Trapper	Duluth, MN	46.897010° N	-91.912430° W	0.85	4/4/18	5/6/18
Outfitter	Grand Marais, MN	47.746960° N	-90.385090° W	0.65	5/7/18	6/20/18

Table 1. Study locations and dates for the spring 2018 season.

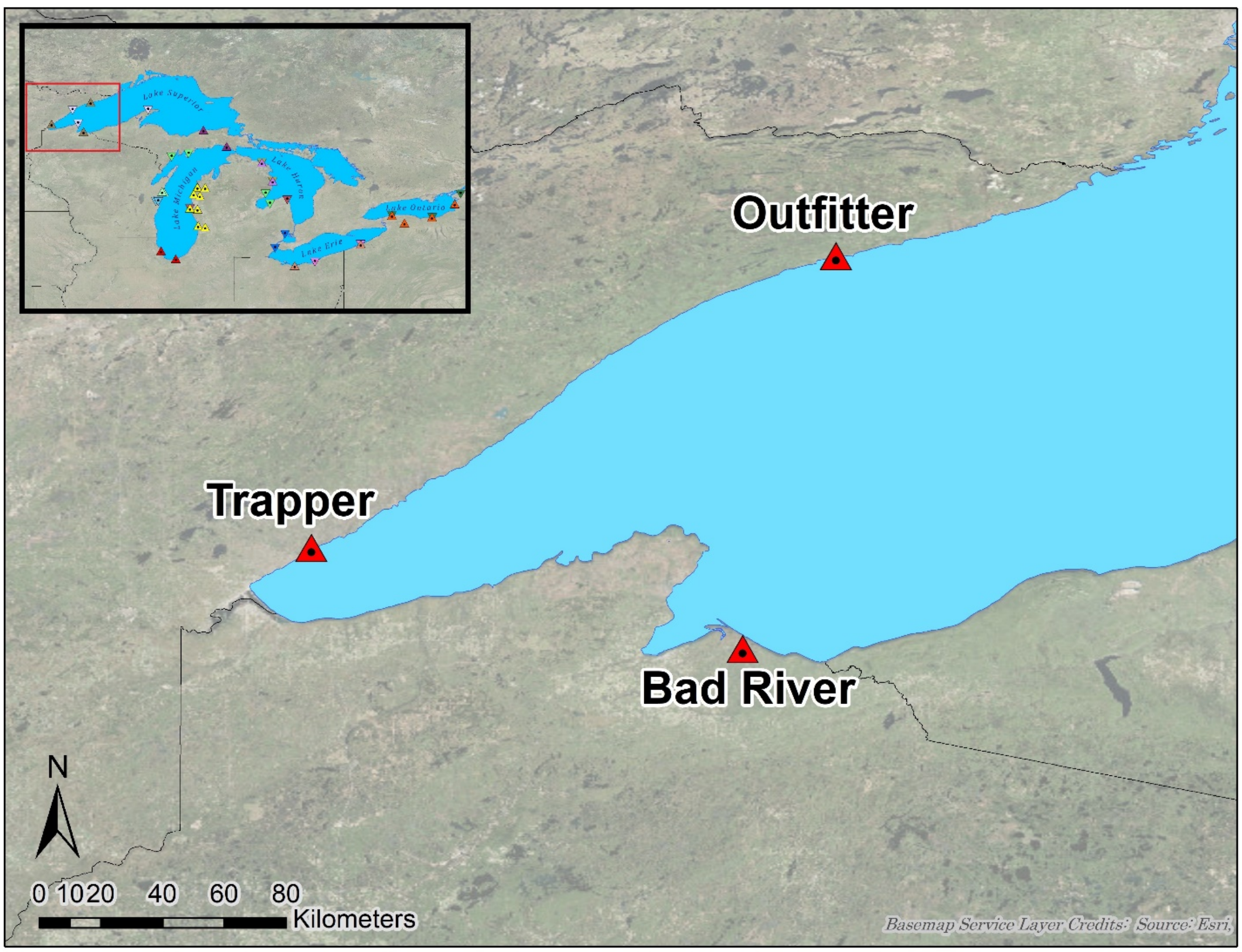

Figure 1. Map of study locations for spring 2018 on Lake Superior.

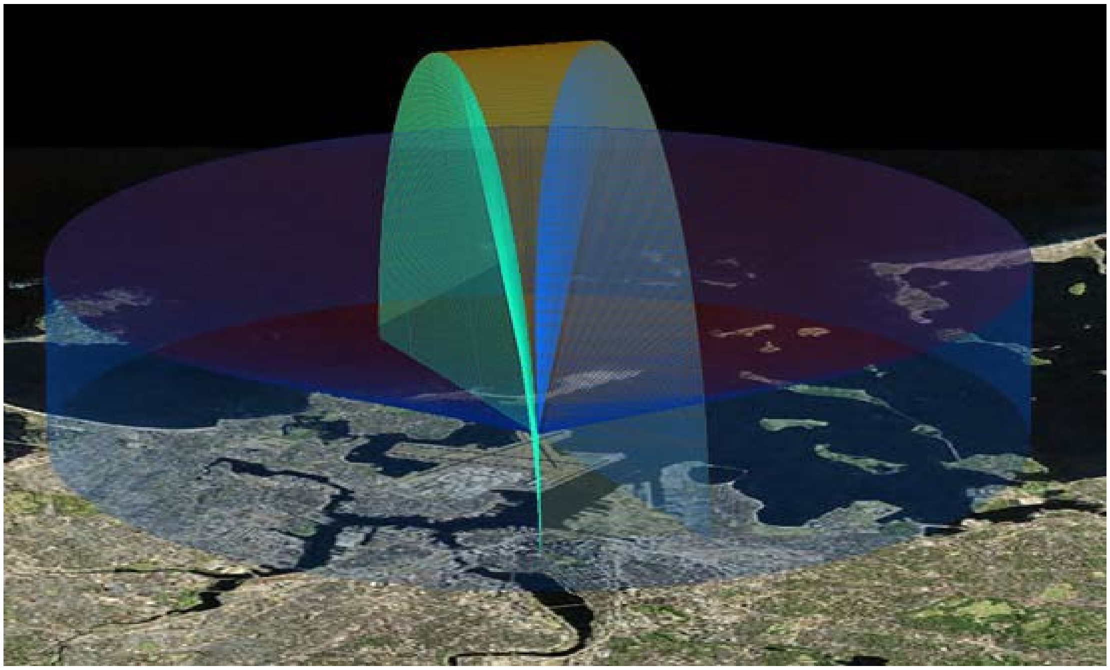

Figure 2. Computer representation of radar scanned volume. This is graphic displays the survey volume scanned by horizontal (blue) and vertical (green) radar antennas used by the U.S. Fish and Wildlife Service during spring 2018. Graphic provided by DeTect, Inc.

Equipment

We used a model SS200DE MERLIN Avian Radar System (DeTect Inc., Panama City, FL) to record migration movements. This system was selected because it is a self-contained mobile unit specifically designed to detect, track, and count bird and bat targets. The system employed two marine radar antennas that operated simultaneously: the horizontal surveillance radar (HSR) scanned the horizontal plane while the vertical scanning radar (VSR) scanned a vertical slice of the sky (Figure 2). Each antenna emanated a fan-shaped beam approximately 25° wide. Both antennas use S-band radar frequencies to enhance detection of birds and bats. This wavelength is less sensitive to insect and weather contamination than X-band (Bruderer 1997). The radars spin perpendicular to each other at a rate of 20 revolutions per minute and synchronized so as not to emit over one another. The HSR antenna was fixed to a telescoping base that was raised to approximately 7 m above ground for operation. This radar rotated in the horizontal plane with a 7° tilt to reduce the amount of ground clutter included within its view. The HSR had an approximate detection range of 3.7 km and the VSR had an approximate detection range of 2.8 km. The HSR was primarily used to provide information on target direction. The VSR provided information on the number of targets and the height of targets.

Radar Setup and Data Collection

We deployed the radar system during the first week of April until the middle of June to capture the 2018 spring migration season. Establishing the radar system at the selected site involved micro-site selection, orienting the VSR, and making adjustments to ensure adequate information was captured and interference from the surrounding landscape was minimized. We anticipated a primarily northbound direction of migration during spring and oriented the VSR to an angle that was slightly off perpendicular to anticipated direction of traffic. This orientation was a compromise between a perpendicular angle that would intercept the greatest number of targets (birds or bats) and a parallel angle that would maximize the amount of travel time within the vertical radar beam.

Bad River Clutter Maps

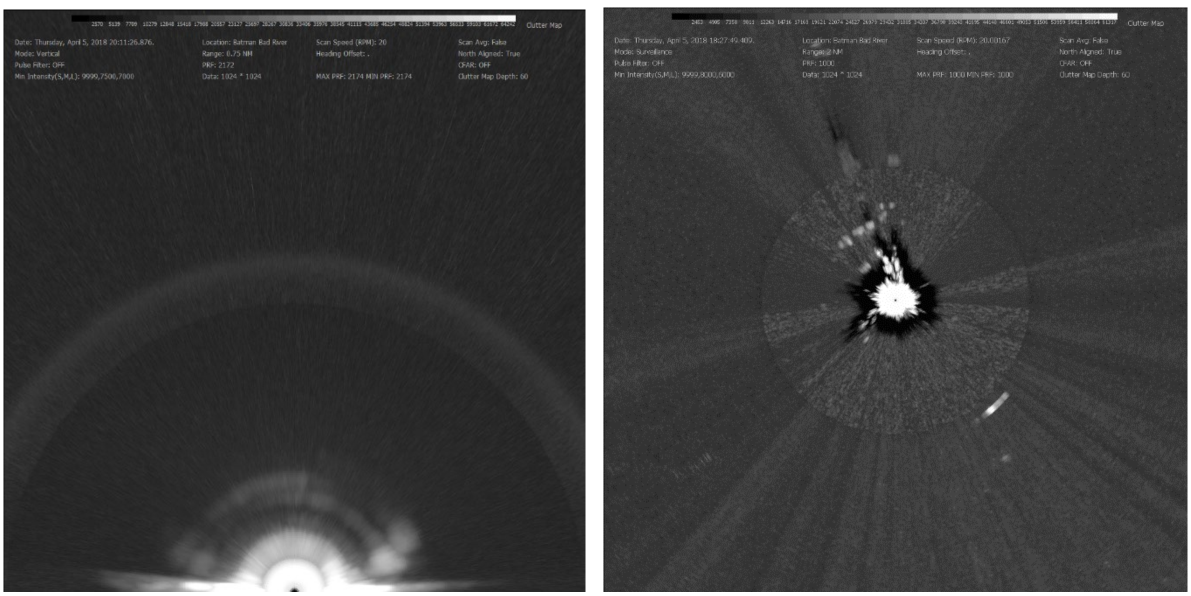

Figure 3. Clutter maps from VSR (left) and HSR (right) at study site on the Bad River Reservation in Wisconsin during the spring 2018 migration season. Brighter areas represent static returns from stationary objects such as tree lines and fencerows, or arcs from irregular radar returns. Detection of targets may be reduced or lost in these areas due to obstruction from these objects.

Trapper Clutter Maps

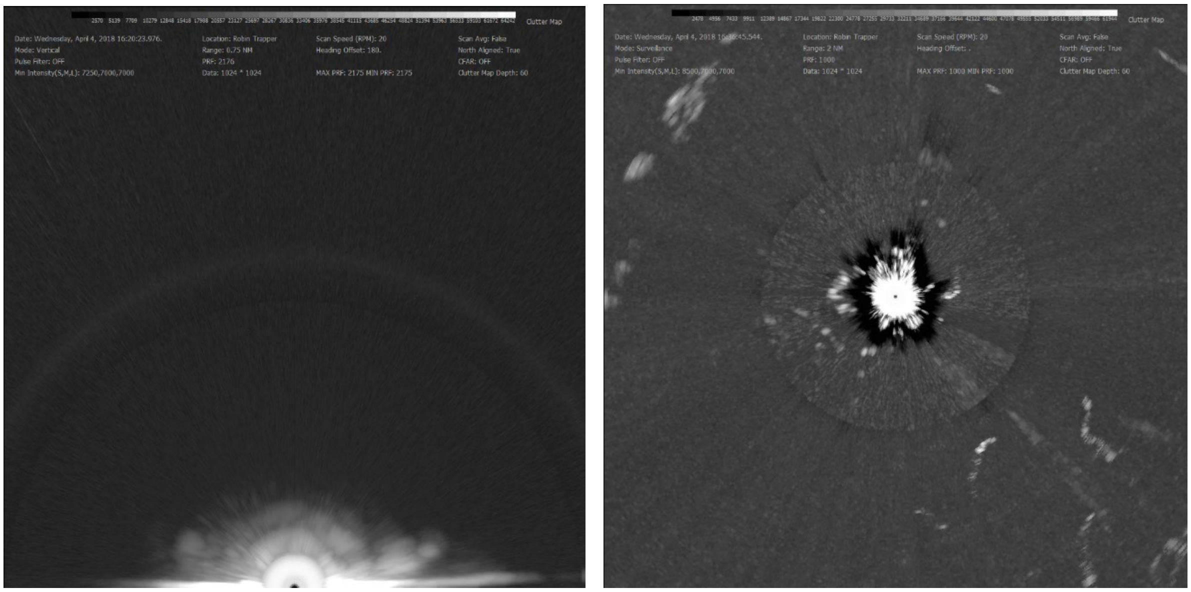

Figure 4. Clutter maps from VSR (left) and HSR (right) at study site near Duluth, MN during the spring 2018 migration season. Brighter areas represent static returns from stationary objects such as tree lines and fencerows, or arcs from irregular radar returns.Detection of targets may be reduced or lost in these areas due to obstruction from these objects.

Outfitter Clutter Maps

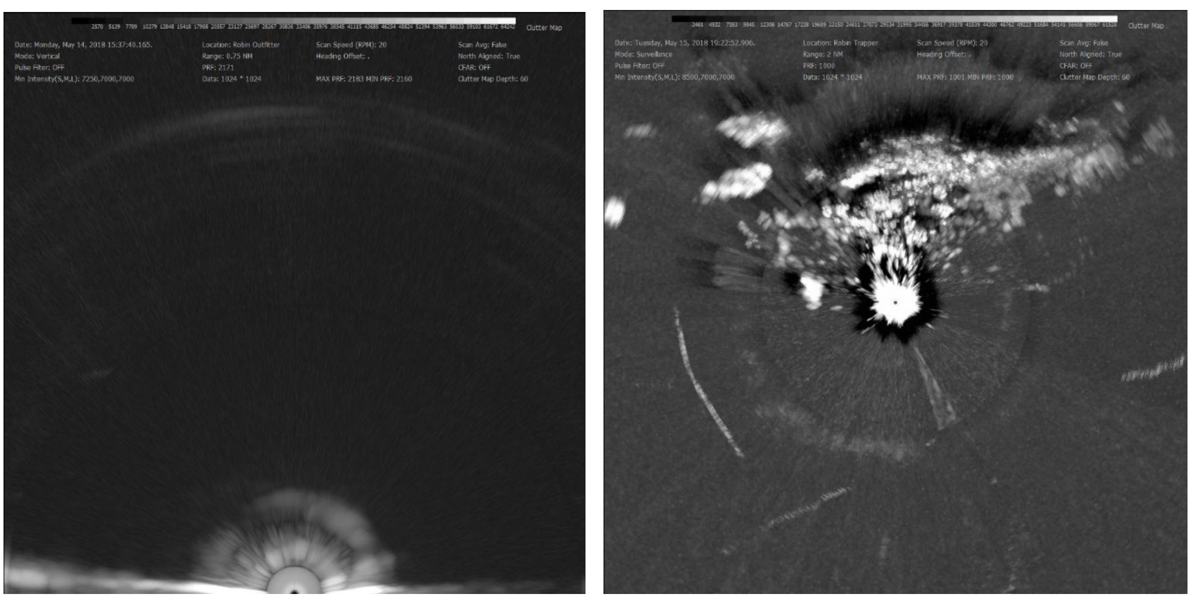

Figure 5. Clutter maps from VSR (left) and HSR (right) at study site near Grand Marais, MN during the spring 2018 migration season. Brighter areas represent static returns from stationary objects such as tree lines and fencerows, or arcs from irregular radar returns. Detection of targets may be reduced or lost in these areas due to obstruction from these objects.

To improve data collection, clutter maps were generated using 60-scan composite images (Figures 3-5) at time periods with low biological activity. These maps identify areas with constant returns (areas that are white), such as tree lines, fencerows and buildings. These objects reduced our ability to detect targets in certain regions of the sample volume, and as a result, those regions were assigned a reflectivity threshold that prevented the constant returns from being included in the data.

Following this initial set up, the MERLIN software from DeTect Inc. was calibrated to site conditions. The MERLIN software provides real-time processing of raw radar data to locate and track targets while excluding non-targets and precipitation. However, parameters used by the tracking software require adjustments to account for site-specific conditions. We established these settings to minimizing inclusion of non-targets while maximizing cohesive tracks of bird and bat targets. We checked these settings periodically during the data collection period to ensure continuous function, monitored raw (unprocessed analog radar returns) and processed radar outputs, and managed data storage. In addition to storing all the processed data, we maintained samples of raw radar data for potential reprocessing.

Radar System Outputs

The MERLIN software records measurements of the target size, shape, location, speed, and direction of movement of each object (potential target) moving through the airspace. Objects detected on a sequence of scans may be classified as a biological "target" by the software and recorded in a database. To reduce potential false tracking, the MERLIN tracking algorithm removes tracks with fewer than five observations. We produced two- dimensional digital displays of targets tracked in real-time and static images of tracked targets over a specified period of time (Trackplots) for both VSR and HSR. During field visits, biologists viewed the real-time digital display to ensure it agreed with the raw radar display. Fifteen-minute Trackplots were also reviewed to assess target direction and height during recent activity and address any issues with persistent clutter.

Data Processing and Quality Control

Prior to data analysis, data processed by MERLIN software were further evaluated for potential contamination by non-targets. We reviewed all data in 15-minute time increments and removed time periods that were dominated by rain. Data were also reviewed for time periods dominated by radar returns caused by insects, waves, or other forms of transient clutter. Once contaminated time periods were removed, we summarized data for further analysis using database queries provided with the radar system by DeTect Inc..

Data Summary and Trends Analysis

Data from the HSR were used to examine the direction of target movements. All targets within the detection radius (3.7 km) were included in the analysis. Data from the VSR were used to calculate target passage rate (TPR), as well as target altitudes. VSR data were truncated to a 1-km "standard front," which is a common metric in radar research (Lowery 1951, Liechti *et al*. 1995, Kunz *et al*. 2007). The standard front is a volume that extends 500 m to either side of the radar and extends vertically up to the maximum height of 2.8 km.

To examine changes over the diel cycle, we calculated sunrise and sunset times and segregated target counts into four biological time periods: dawn, day, dusk, and night. We defined dawn as 30 minutes before sunrise to 30 minutes after sunrise, day as 30 minutes after sunrise to 30 minutes before sunset, dusk as 30 minutes before sunset to 30 minutes after sunset, and night as 30 minutes after sunset to 30 minutes before sunrise.

Temporal Trends

We plotted counts of targets per hour for both HSR and VSR antennas as a time series to identify pulses of nocturnal activity, season duration, and changes in patterns of activity over time. The HSR and VSR radars have different strengths that complement one another. Counts from both antennas are viewed as indices of target movement, and were plotted together. The HSR has a larger sample volume and generally tracks lower-flying targets in a 360˚ span around the radar unit. HSR detection is not affected by target flight direction, but it is much more affected by ground clutter than the VSR. Ground clutter, along with the shape of the HSR sample volume, can cause both under- and over-counting. Targets blocked from view by ground clutter may not get counted, and targets that fly into and out of areas with clutter may get counted multiple times. Consequently, HSR counts are more heavily influenced by surrounding site conditions than VSR counts. HSR can provide a better description of target activity under certain conditions, however, such as when targets are primarily at low elevation. The VSR index is a more reliable indicator of target passage through the standard front. The vertical sample volume is mostly unimpeded by clutter, except in the lowest altitude bands. VSR detection rates are likely affected by target direction, and vary with distance from the radar (Bruderer 1997, Schmaljohann *et al*. 2008). Plotting these indices together provided a more comprehensive view of changes in target activity over time.

Directional Trends

We analyzed flight directions following methodology for circular statistics (Zar 1999) provided within DeTect's queries. We used radial graphs to plot the number of targets per 8-cardinal directions (N, NE, E, SE, S, SW, W, NW) during four biological time periods (dawn, day, dusk, night). Additionally, we used the circular mean direction of targets each night to examine potential origins of migrants, plotting the estimated direction of origination as a line with length representing the magnitude of migration. This measure does not indicate variance of directionality, which can be large, but does provide a visualization of the likely origin direction of many migrants.

Altitudinal Trends

VSR data include the estimated altitude of each tracked target within the standard front. However, the size and shape of the radar beam changes with altitude, producing a smaller sample volume at low altitudes and a larger sample volume at high altitudes. To address this, we calculated the volume of the radar beam within each 50-m altitude band by Monte Carlo integration (Figure 6; Press, Teukolsky, Vetterling, and Flannery 2007), and adjusted counts within each band to provide a more accurate representation of migrant density by altitude. We report density of targets per 1,000,000 m^3 per hour for each biological period. For more detail, see Rathbun *et al*. 2016.

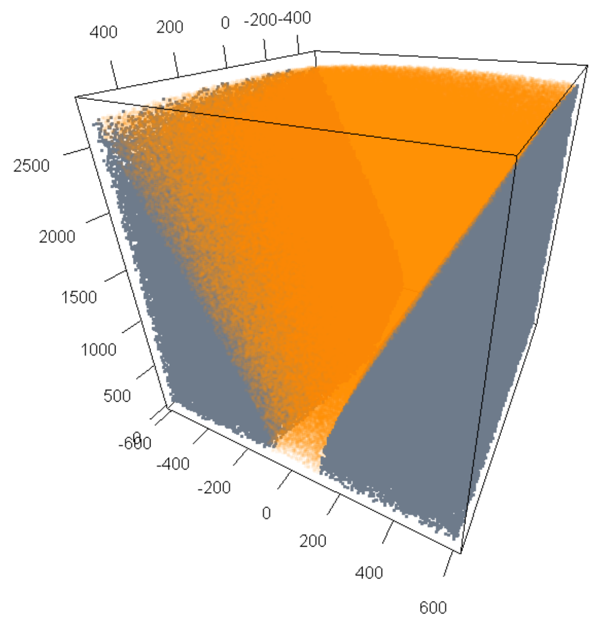

Figure 6. Graphical representation of the structural volume of the VSR within the standard front used to estimate radar sample volume per 50 m altitude band. In this graphic the radar unit is located at the origin and the radar beam extends to 500 m on either side of the radar unit and up to a maximum height of 2800 m. The orange semi-transparent points represent the volume contained by the structure of the radar beam. Dark gray points represent the volume that is within the box but are not included in the volume of the radar beam.

RESULTS

Temporal Trends

Figures 7-9 (below) show the target counts from the radar units' vertical and horizontal antennas for each hour over the entire season. These two antennas sample different areas of the airspace and at different ranges; in general we use the VSR counts as a more reliable, albeit conservative, estimate of migratory activity. Gaps in the lines represent hours with data missing, due to radar downtime for maintenance or malfunction, or due to the data being removed due to contamination from large amounts of clutter such as rain, insects, or waves. Vertical lines represent midnight on the specified date, and the night starts on the previous day, generally indicated by the rise in migrant counts.

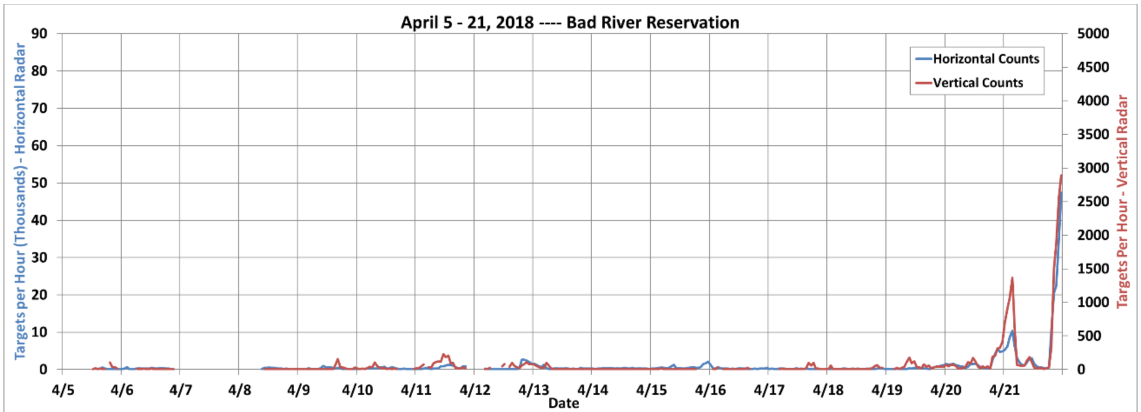
April 5 - 21, 2018 ---- Bad River Reservation
Targets per Hour (Thousands) - Horizontal Radar
Targets Per Hour - Vertical Radar
Horizontal Counts
Vertical Counts
Date
4/5
4/6
4/7
4/8
4/9
4/10
4/11
4/12
4/13
4/14
4/15
4/16
4/17
4/18
4/19
4/20
4/21

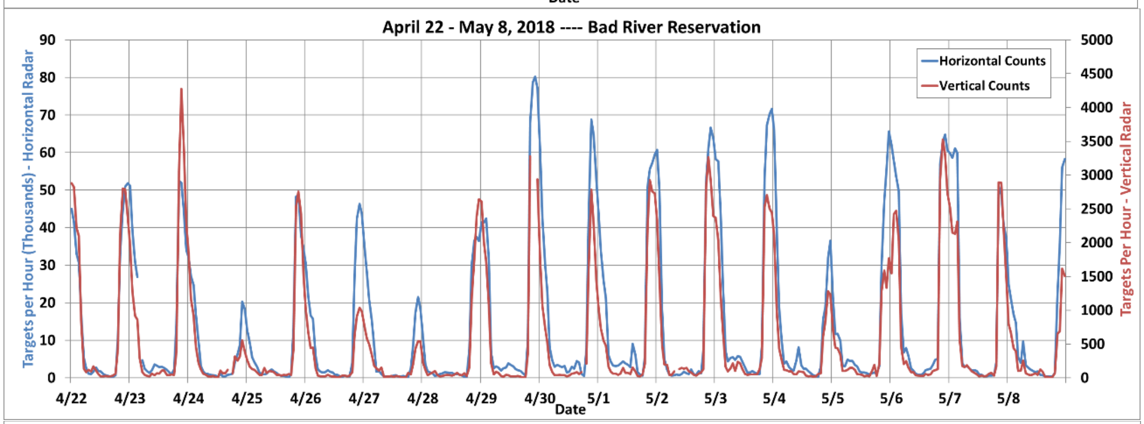
April 22 - May 8, 2018 ---- Bad River Reservation
Targets per Hour (Thousands) - Horizontal Radar
Targets Per Hour - Vertical Radar
Horizontal Counts
Vertical Counts
Date
4/22
4/23
4/24
4/25
4/26
4/27
4/28
4/29
4/30
5/1
5/2
5/3
5/4
5/5
5/6
5/7
5/8

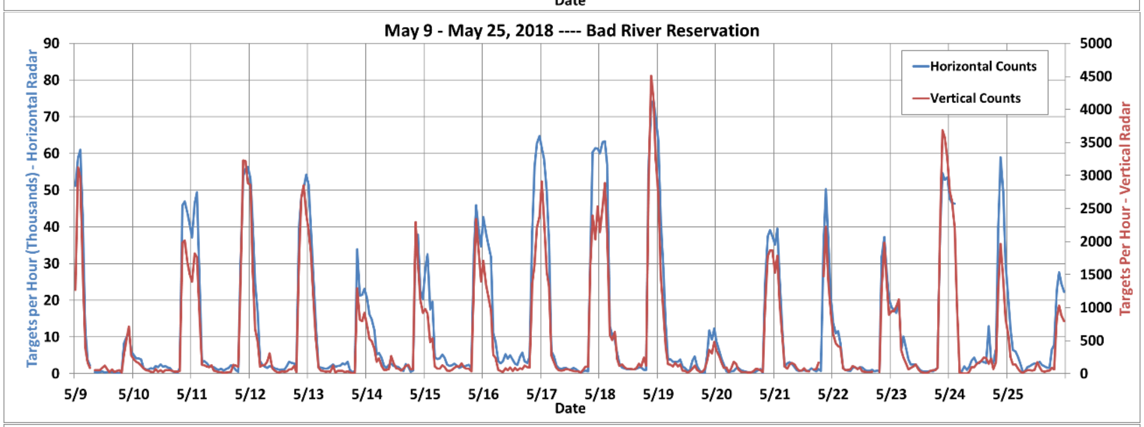
May 9 - May 25, 2018 ---- Bad River Reservation
Targets per Hour (Thousands) - Horizontal Radar
Targets Per Hour - Vertical Radar
Horizontal Counts
Vertical Counts
Date
5/9
5/10
5/11
5/12
5/13
5/14
5/15
5/16
5/17
5/18
5/19
5/20
5/21
5/22
5/23
5/24
5/25

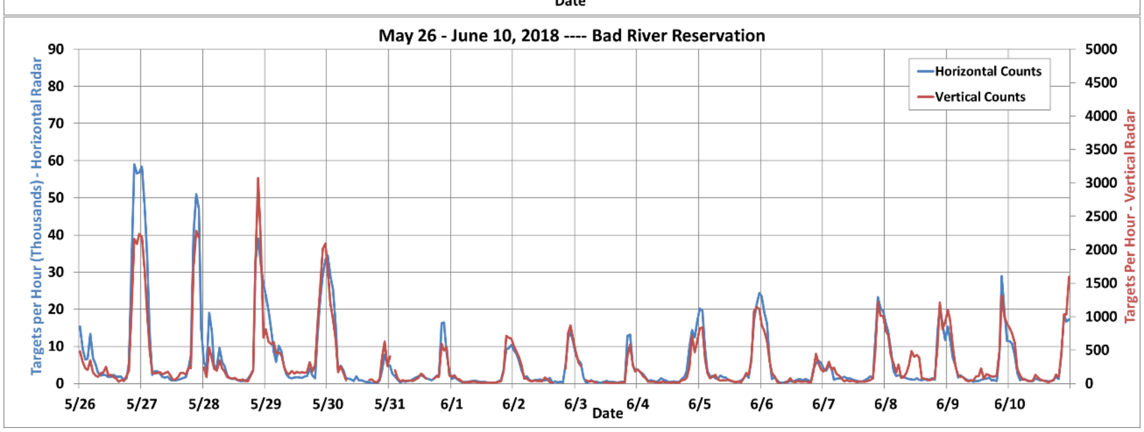
May 26 - June 10, 2018 ---- Bad River Reservation
Targets per Hour (Thousands) - Horizontal Radar
Targets Per Hour - Vertical Radar
Horizontal Counts
Vertical Counts
Date
5/26
5/27
5/28
5/29
5/30
5/31
6/1
6/2
6/3
6/4
6/5
6/6
6/7
6/8
6/9
6/10

Figure 7. (Previous Page) Time series of horizontal and vertical target counts for Bad River. The horizontal (HSR) counts (blue) are plotted on the left y-axis with the vertical (VSR) radar counts (red) plotted against the right y-axis, both on the scale of targets per hour. In early spring, there was little migratory movement at the Bad River Reservation up through April 22nd. This start date was likely influenced due to a late April snow storm in the area that only melted fully around April 22nd. Without the snow, it is likely that migrants would have arrived earlier, though perhaps not all at the same time. After migration started, movement occurred on almost every night up through May 30th, at which point it dropped off dramatically.

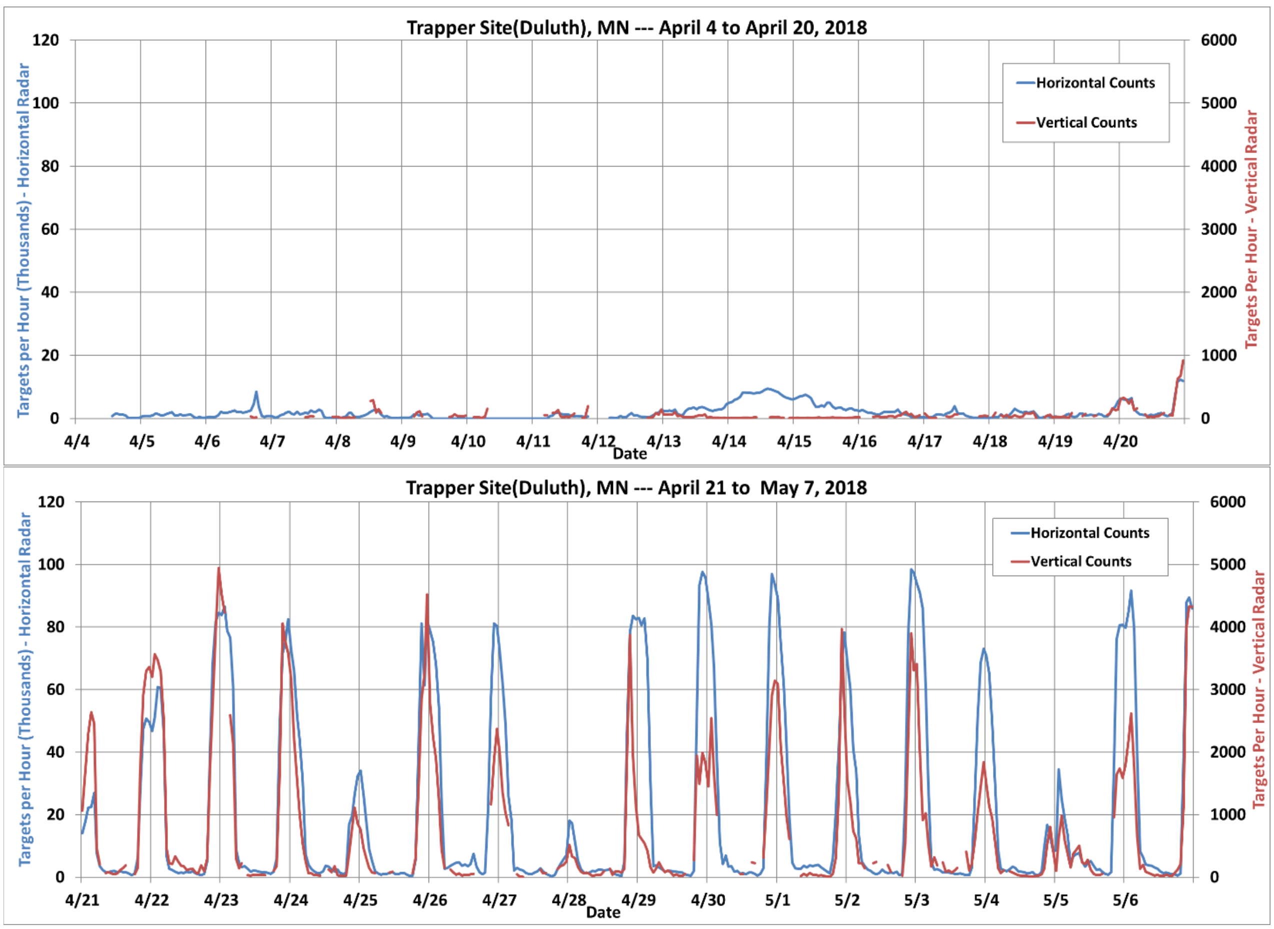

Figure 8. Time series of horizontal and vertical target counts for Trapper. The horizontal (HSR) counts (blue) are plotted on the left y-axis with the vertical radar (VSR) counts (red) plotted against the right y-axis, both on the scale of targets per hour. Near Duluth, MN, for the first half of the 2018 Spring season, patterns were very similar to the site at Bad River, WI (Figure 7). Migration started on 4/21 after the snow had melted and continued almost every night through 5/7 when we relocated the radar unit.

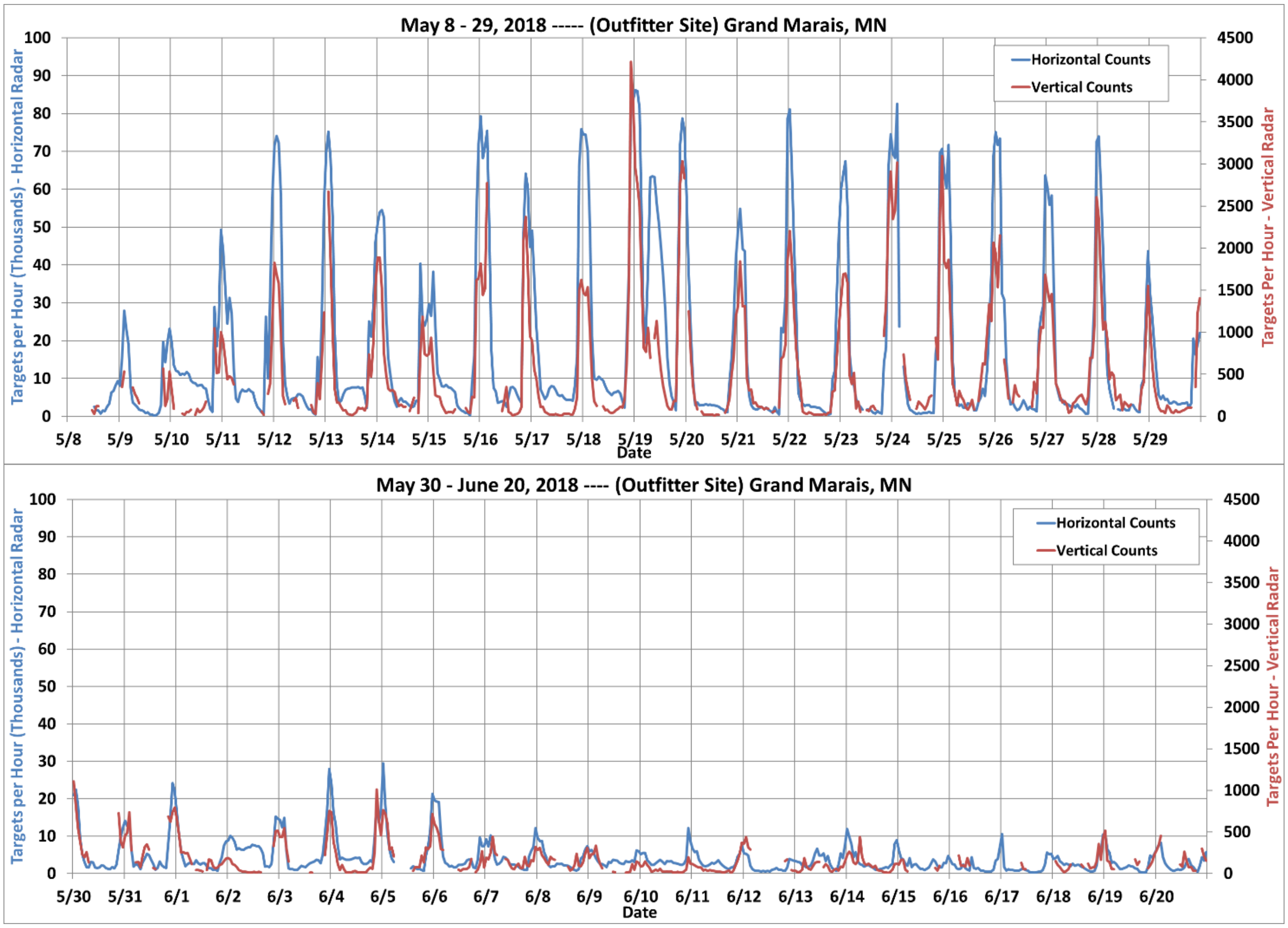

Figure 9. Time series of horizontal and vertical target counts for Outfitter. The horizontal (HSR) counts (blue) are plotted on the left y-axis with the vertical radar (VSR) counts (red) plotted against the right y-axis, both on the scale of targets per hour. Near Grand Marais, MN at the Outfitter Site for the second part of the Spring 2018 season, activity was similar to Bad River, WI (Figure 7) but with some potentially important differences. We moved the radar unit to this site on May 8th, and observed little migration for the first 3 nights at this location. This could have been a lull in migration, or could have represented a late arrival of migrants to the area, especially due to the northern latitude of this site. After May 12th, the similarities between Bad River and the Outfitter site were much stronger. Migration seemed to end around May 30th, with little movement afterwards, presumably due to migrants already moving through and being on their breeding grounds.

Directional Trends

Direction by Biological Period

Bad River

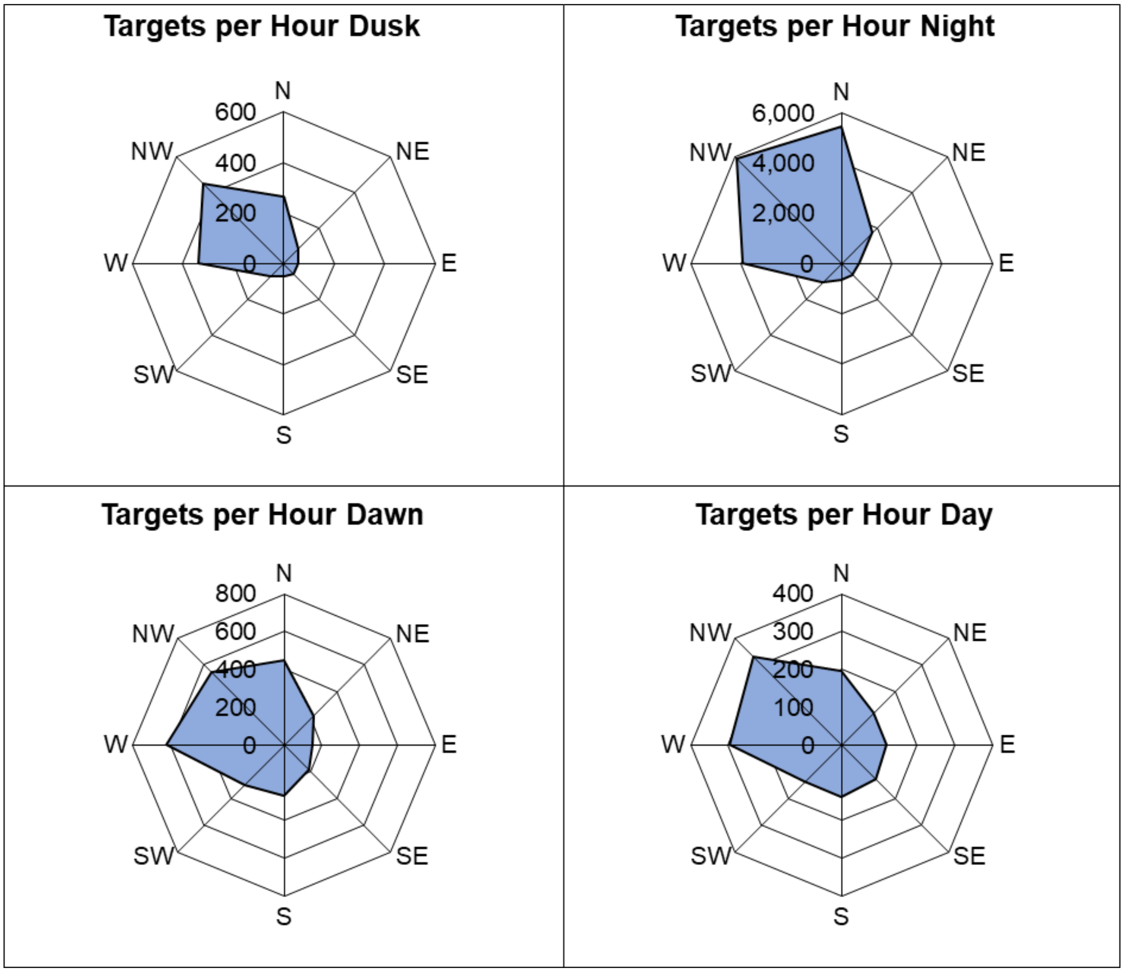

Figure 10. Rose graphs showing the movement direction of targets during the four biological time periods at Bad River. The measures are in targets per hour, as there are a different number of hours in each biological time period. Note the different scales between the graphs, as the dimensions of the blue polygon are meant to illustrate differences in behavior and movement direction and not illustrate differences in activity levels.

Overall, directionality was relatively consistent among biological periods at the Bad River site, with the primary direction of movement to the north, northwest, or west. Migrants moved predominately to the northwest at dusk. This directional movement is consistent with navigation towards the Bayfield Peninsula. Additionally, there was also movement to the west, heading along the lakeshore and possibly to go around the western end of Lake Superior. At night, migrants continued to move predominately northwest and north. These migrants may have been navigating to the Apostle Islands, or heading to attempt an open water crossing of Lake Superior. At dawn, the highest proportion of migrants was oriented to the west, suggesting migrants may be less inclined to cross or be over the water during the dawn period. Indeed, there was a higher proportion of migrants headed back in towards shore, to the south and southeast, at dawn than during the other migratory periods. During the day, directional movement was to the northwest and west, but there were many fewer targets, indicating that this may have been local movement or diurnal migrants such as raptors.

Trapper

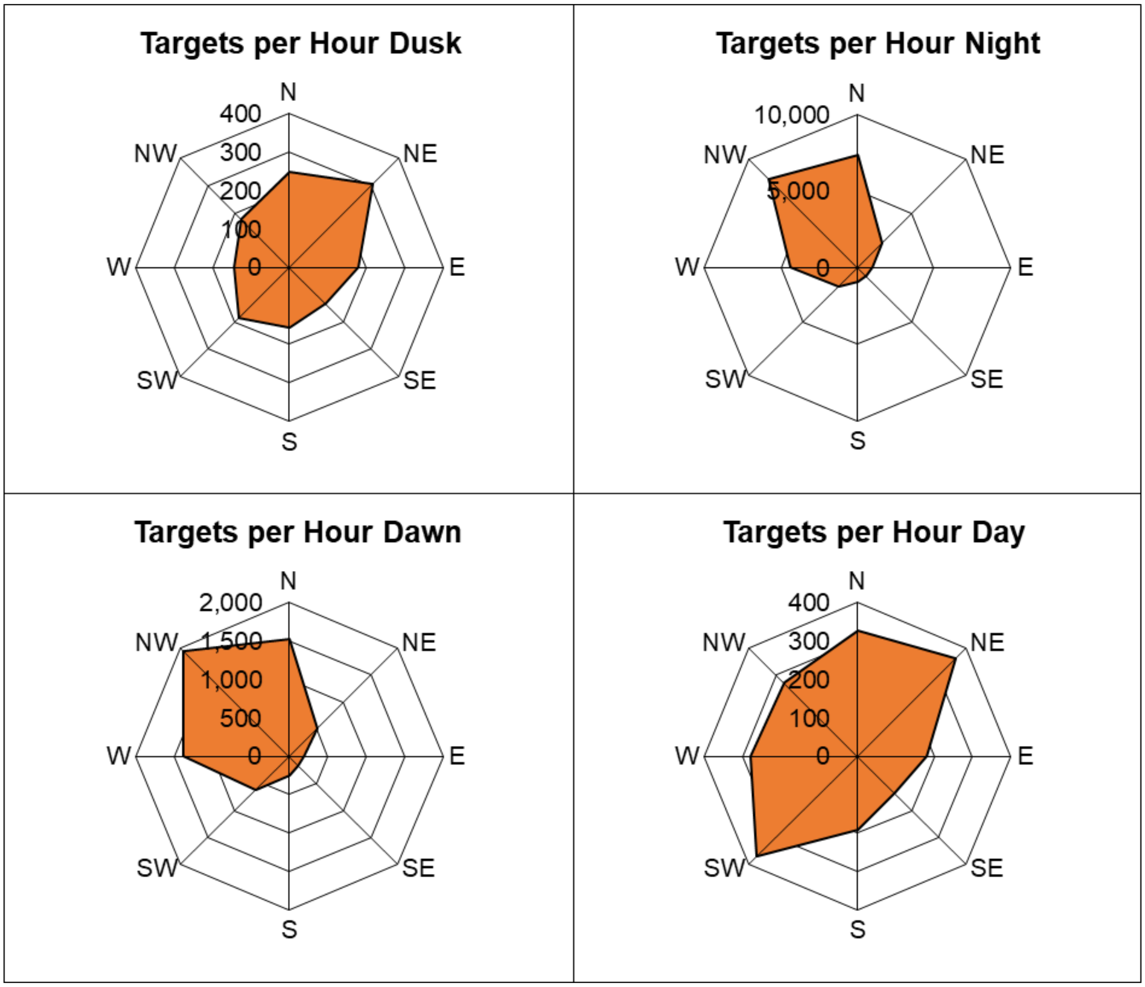

Figure 11. Rose graphs showing the movement direction of targets during the four biological time periods at Trapper. The measures are in targets per hour, as there are a different number of hours in each biological time period. Note the different scales between the graphs, as these are meant to illustrate differences in behavior and movement direction and not illustrate differences in activity levels.

Directional variation among biological periods was greater at Trapper, with heavy movement in the direction of migration (north and northwest) during night and dawn, and substantial shoreline movement (northeast and southwest) during day and dusk. To start their migration, migrants predominately followed along the lakeshore to the northeast at dusk, although there were also substantial southwestern and northern directional components. At night, the migration direction shifted to the north and northwest. This is consistent with the pattern that suggests migrants are predominately crossing over Lake Superior at night, especially on this shorter distance crossing route, effectively 'cutting the corner' of the lake. At dawn, migrants had been flying out over the lake shifted their direction slightly to move directly in towards shore. This is consistent with a dawn turn to shore where migrants attempt to avoid danger from predators and land to rest and refuel (Heist *et al.* 2018). During the day, the activity was along the lakeshore, indicating potential diurnal movement of migrants but likely also the local movement of residents such as gulls foraging along the lakeshore.

Outfitter

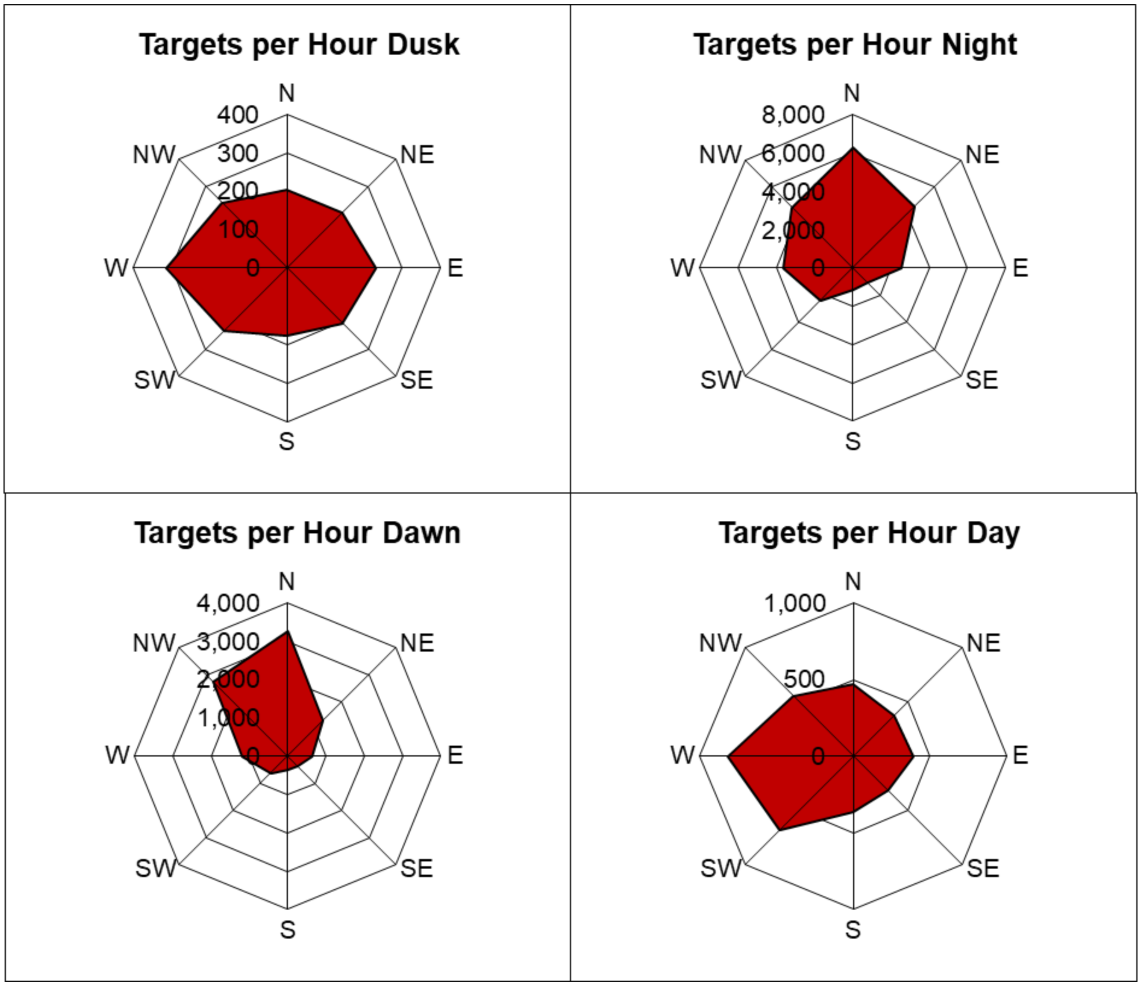

Figure 12. Rose graphs showing the movement direction of targets during the four biological time periods at Outfitter. The measures are in targets per hour, as there are a different number of hours in each biological time period. Note the different scales between the graphs, as these are meant to illustrate differences in behavior and movement direction and not illustrate differences in activity levels.

Similar to Outfitter, night and dawn movement at Trapper was more concentrated, whereas day and dusk movement were less focused. At dusk, movement was omnidirectional, possibly due to a mixture of migrant and non-migrant activity. At night, however, there was strong movement towards the north. This supports the hypothesis that migrants were likely crossing over Lake Superior. There is also a substantial subset of migrants moving to the northeast, either due to migrants following the shore from the southwest, or continuing along the shore after crossing the lake. At dawn, migrants move to the north and northwest, consistent with migrants over water moving directly to shore.

Example Migration Trackplots

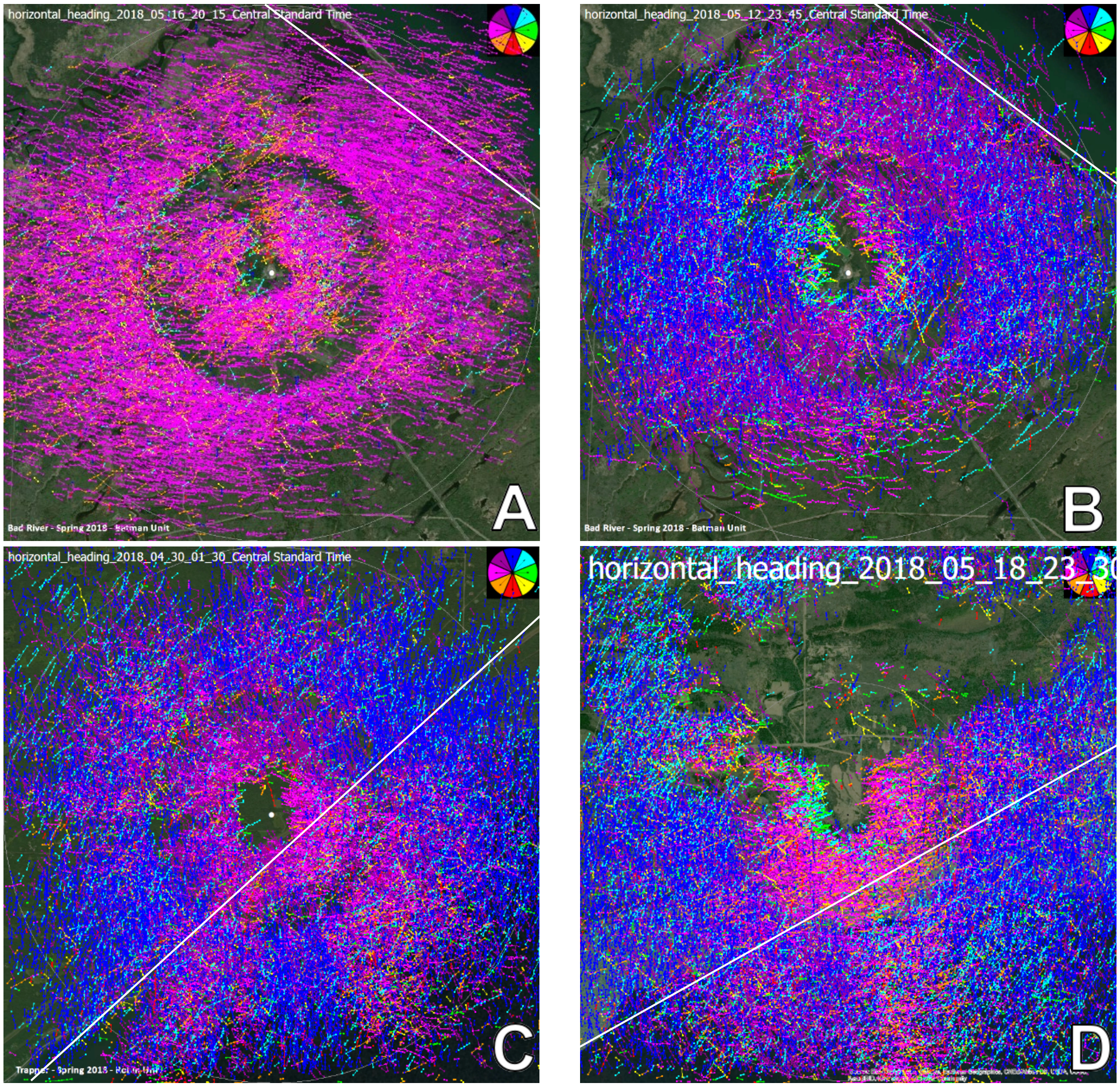

Figure 13: Examples of migration around Lake Superior. Each colored line is a tracked migrant, with color indicating direction, as noted in the color-coded compass rose in the upper right corner of each figure (N=Blue, E=Green, S=Red, W=Purple). The white point in the center of each panel denotes the location of the radar unit, while the white line denotes the approximate location of the shoreline. Each panel depicts a 15-minute interval of time, starting at the time referenced at the top of each panel.

A. **High numbers of migrants moving predominately due west at Bad River, WI following along the shoreline of Lake Superior. Lake Superior is to the NE. (May 16, 20:15)**
B. **High numbers of migrants moving predominately north at Bad River, WI , but with some westward movement too, mainly heading out over Lake Superior. Lake Superior is to the NE. (May 12, 23:45)**
C. **High numbers of migrants moving north, coming across Lake Superior at the Trapper site near Duluth, MN. Lake Superior is to the SE. (April 30, 01:30)**
D. **Migrants arriving at the north shore of Lake Superior near Grand Marais at the Outfitter site, mainly heading north. The large blank spot to the north is due to clutter from a large tree lined hill near the radar unit that obscured the radar unit's detection ability, and not due to a lack of migrants in that area. Lake Superior is to the SE. (May 18, 23:30)**

Direction of Origin

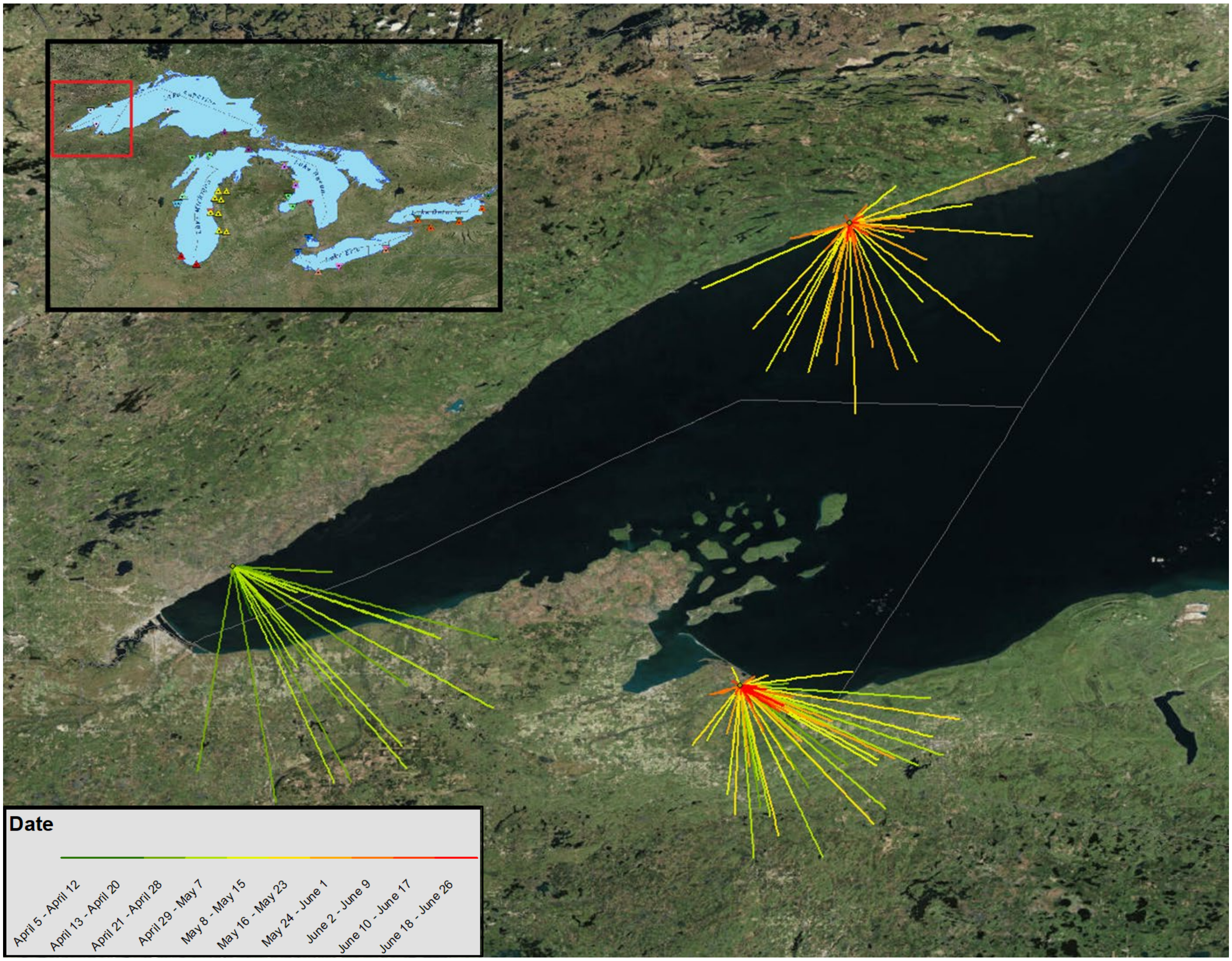

Figure 14. Estimated direction of origin each night. Lines represent the estimated direction of migrant origin and magnitude of movement each night of the spring 2018 season. The angle of each line is the circular mean of target headings, represented as movement toward the radar unit. Line length is proportional to the number of targets detected on the HSR each night. Night was defined as 30 minutes after sunset to 30 minutes before sunrise. Date is represented by color, with warmer colors later in the season and greener colors earlier in the season.

Figure 14 depicts movement by night at each of the sites. Each line depicts a night, with angle providing mean direction of movement for that night from origin to site. Color indicates date (indicated by color of the line) and HSR target count (indicated by length of the line). Most movement at Bad River, WI and Trapper (Duluth, MN), originated from the south to southeast. At Bad River, this is consistent with migrants approaching the lake, then orienting to the Bayfield Peninsula, the Apostle Islands, or following along the coastline to the west. At Trapper, near Duluth, MN, the directional pattern indicates migrants that are crossing over corner of the lake, rather than going around the end of the lake when they arrived from the southeast. At Outfitter, near Grand Marais, MN, there was more variation in migrant direction. The highest concentration of movements is consistent with an origination direction from the Bayfield Peninsula and the Apostle Islands. If migrants are originating in these areas it would indicate they crossed 45 miles (75 km) of open water before arriving at the north shore. Other lines show that movement occasionally came from other areas, such as the Keweenaw Peninsula, potentially showing an even greater open water crossing of 80-90 miles (125-150 km).

Lines do not indicate that all or even most migrants are moving in the same direction. Flight directions have substantial variation at night, as depicted in Figures 10-12. The line indicates the “typical” direction of flight by averaged headings among all migrants. HSR target numbers (length of line) provide a relative measure of migration intensity, but should not be interpreted as the number of migrants passing. This is due to HSR target numbers potentially being inflated due to double-counting (see Methods). Generally, short lines represent relatively low-activity nights and long lines represent high-activity nights.

Altitudinal Trends

During all biological periods, the highest densities of targets were at low altitudes, and most within the rotor swept zone. Other potential heights of interest are many other man-made structures, such as communication towers and buildings. Each of these altitude density distributions also illustrates that mean and median height are not adequate representations of target altitude. An upward skew in target flight heights will result in means and medians that incorrectly imply that the bulk of migrants are traveling at higher altitudes than they actually are. All of our density graphs show the importance of reporting a full altitudinal distribution curve, rather than summary statistics such as mean and median flight height.

Altitude by Biological Period
Bad River, WI

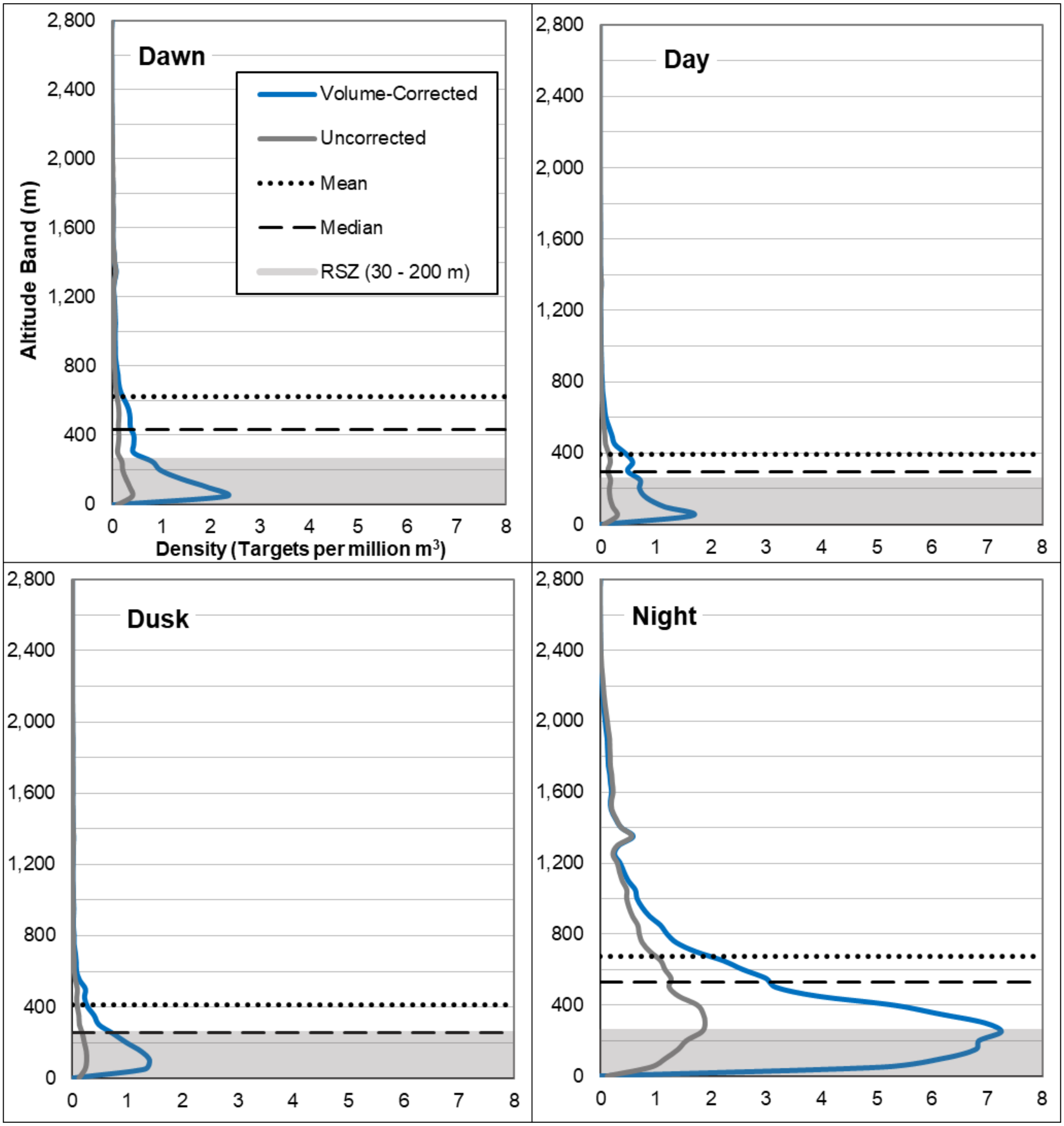

Figure 15. Altitude distribution by biological time period for Bad River. These graphs show the uncorrected (gray) and corrected (blue) density estimates of targets moving on the VSR at different altitudes during the four biological time periods. The mean height for the time period is shown in a dotted line and the median height is shown in a dashed line. A shaded area represents a 30-200 m rotor-swept zone (RSZ). These densities are corrected to account for the differences in sample volume between different altitude bands (see Methods). Note the overall larger numbers/density of migrants moving during the nighttime hours as compared to the other periods. Altitude distributions also indicate seasonal totals, and do not account for differences in flight altitude on particular nights.

Trapper Site, Duluth, MN

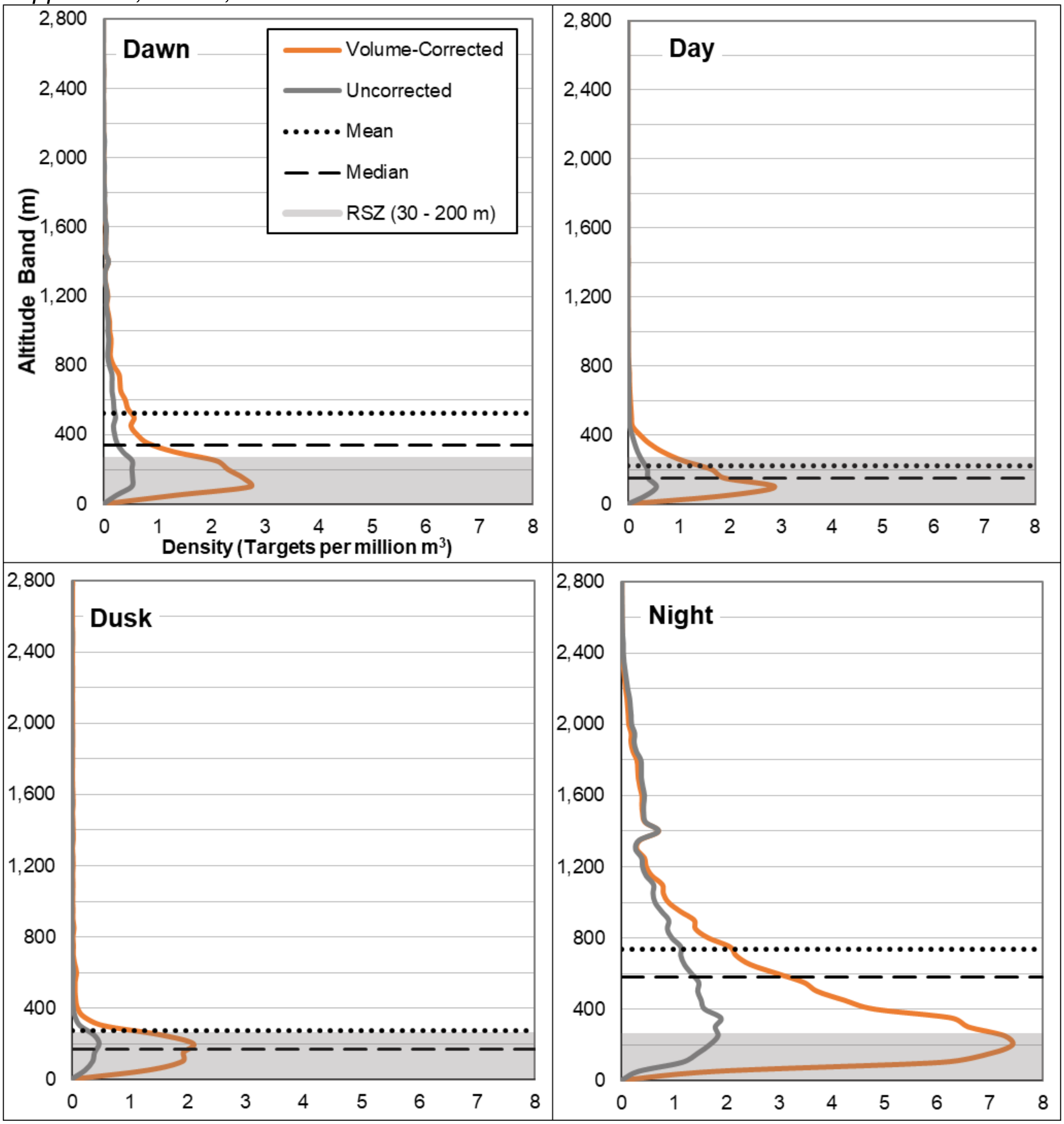

Figure 16. Altitude distribution by biological time period for Trapper. These graphs show the uncorrected (gray) and corrected (blue) density estimates of targets moving on the VSR radar at different altitudes during the four biological time periods. The mean height for the time period is shown in a dotted line and the median height is shown in a dashed line. A shaded area represents a 30-200 m rotor-swept zone (RSZ). These densities are corrected to account for the differences in sample volume between different altitude bands (see Methods). Note the overall larger numbers/density of migrants moving during the nighttime hours as compared to the other periods. Altitude distributions also indicate seasonal totals, and do not account for differences in flight altitude on particular nights.

Outfitter Site, Grand Marais, MN

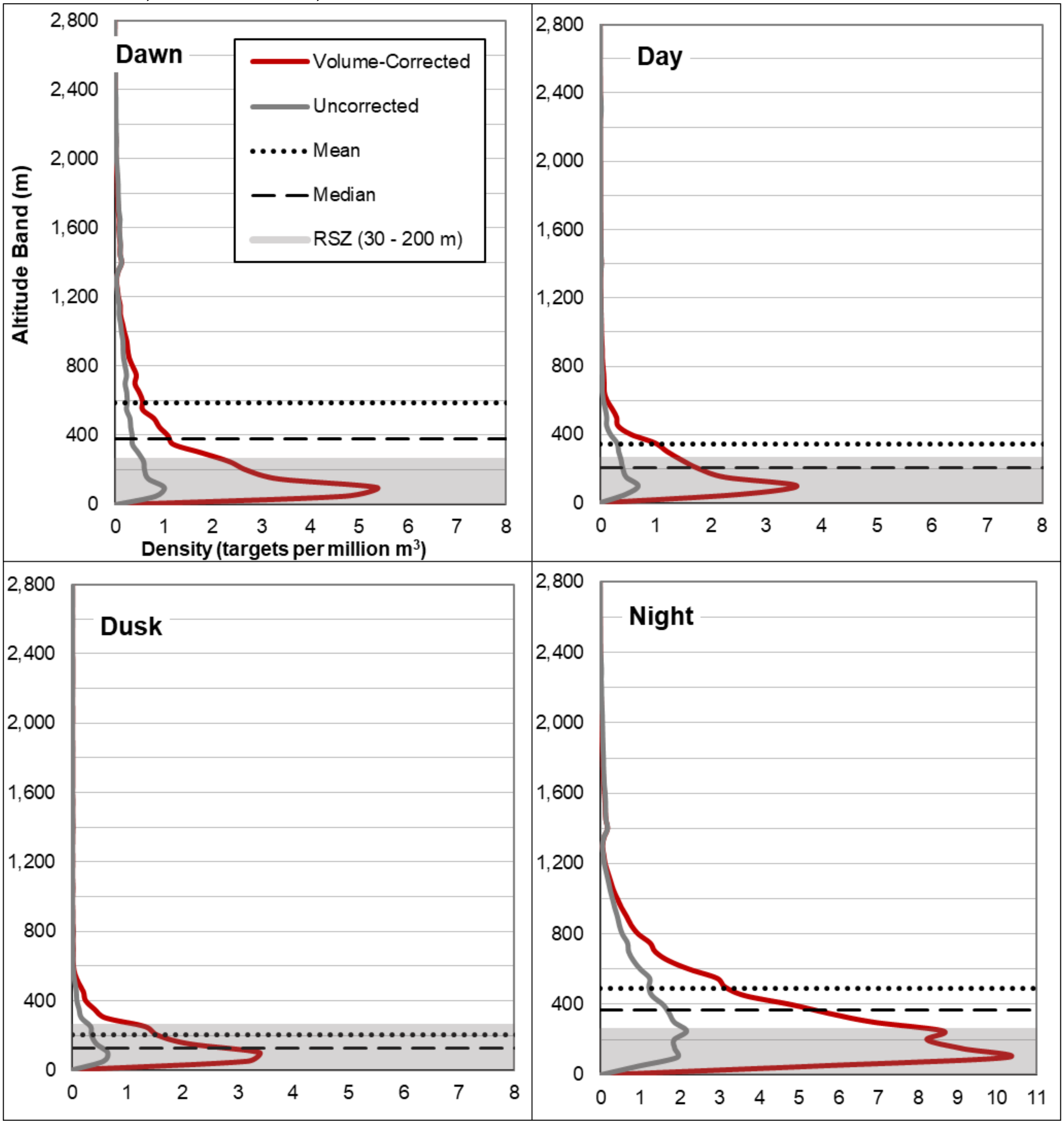

Figure 17. Altitude distribution by biological time period for Outfitter. These graphs show the uncorrected (gray) and corrected (blue) density estimates of targets moving on the VSR radar at different altitudes during the four biological time periods. The mean height for the time period is shown in a dotted line and the median height is shown in a dashed line. A shaded area represents a 30-200 m rotor-swept zone (RSZ). These densities are corrected to account for the differences in sample volume between different altitude bands (see Methods). Note the overall larger numbers/density of migrants moving during the nighttime hours as compared to the other periods. Altitude distributions also indicate seasonal totals, and do not account for differences in flight altitude on particular nights.

Target Density by Altitude and Hour

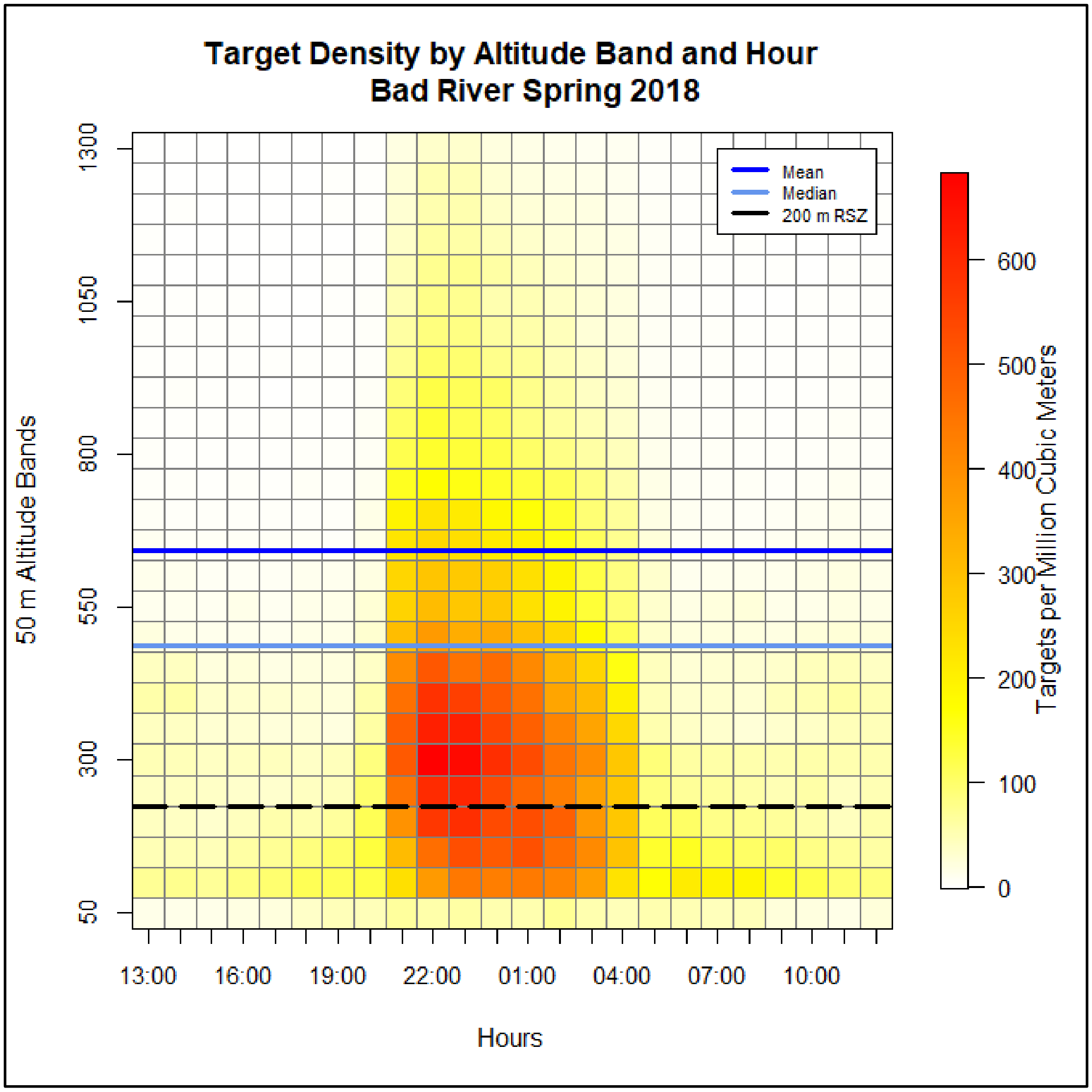

Figure 18. Hourly altitude heat map for Bad River. The Y-axis depicts altitude in 50-meter bands, and the X-axis shows the hour, with midnight (0:00) as the midpoint of the axis. Cell colors depict density of migrants, corrected for radar beam shape, with warmer colors indicating higher target density. Uncorrected mean and median altitudes are depicted in dark and light blue lines, respectively. A 200 m rotor-swept zone is depicted by the dotted black line. The radar units sampled much higher than this 1300-m graph goes, but the bulk of the migrants moved in these lower altitudes, so ranges above 1300-m were not displayed.

Movement densities on this graph depicted by hour of the day and show the onset and decline of migration. There is some movement throughout the day at low densities but around 21:00 migration starts as birds and bats start moving. Initially, migrants fly at a higher altitude, likely to direct their navigation. By 22:00 migrants are flying lower, with the highest densities between 450 and 50m. As the night progresses, both the altitude and overall densities both decrease, and migrant activity declines after 04:00.

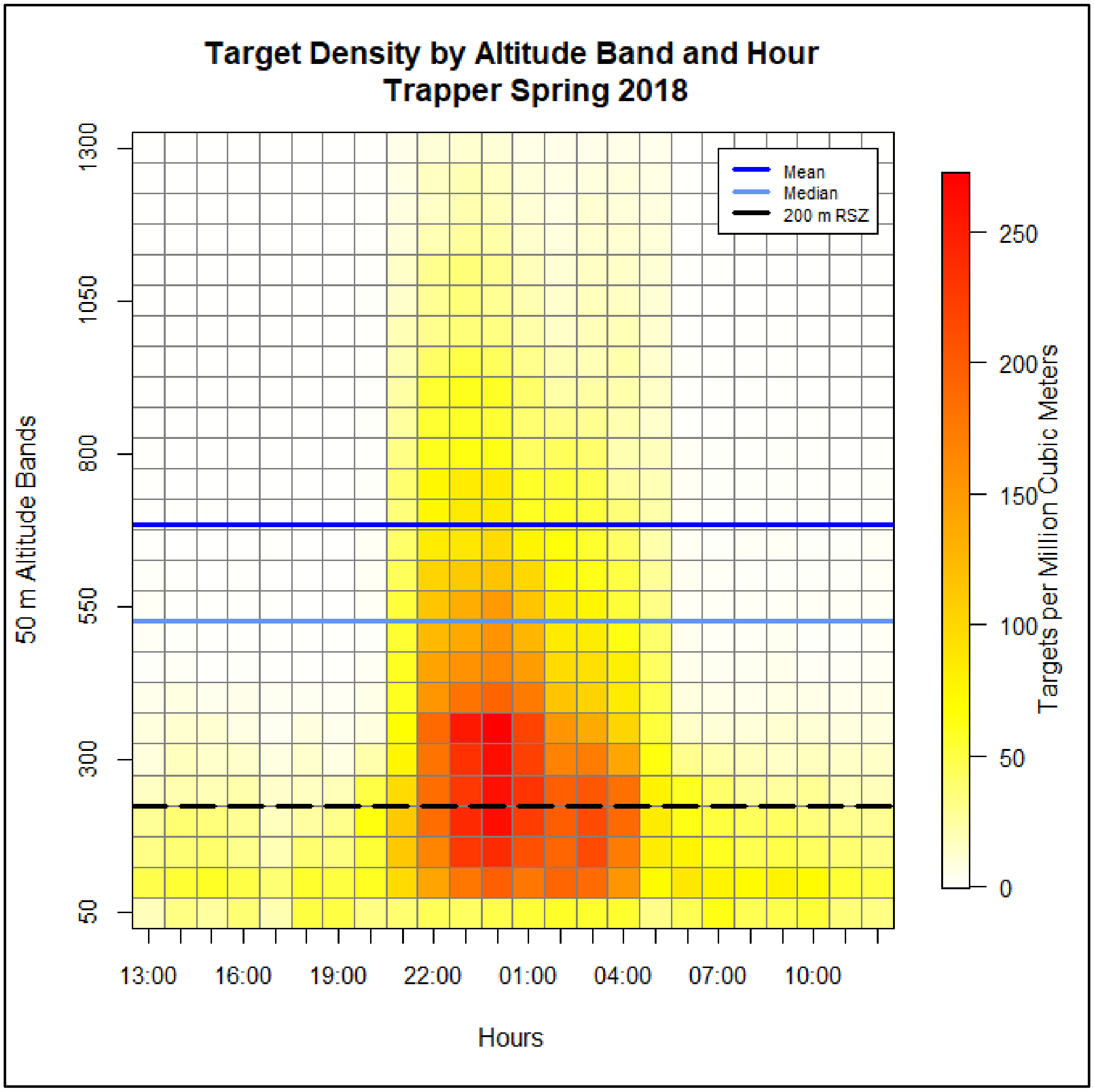

Figure 19. Hourly altitude heat map for Trapper. The Y-axis depicts altitude in 50-meter bands, while the X-axis shows the hour, with midnight (0:00) as the midpoint of the axis. Cell colors depict density of migrants, corrected for radar beam shape, with warmer colors indicating higher target density. Uncorrected mean and median altitudes are depicted in dark and light blue lines, respectively. A 200 m rotor-swept zone is depicted by the dotted black line. The radar units sampled much higher than this 1300-m graph goes, but the bulk of the migrants moved in these lower altitudes, so ranges above 1300-m were not displayed.

A similar pattern to Bad River (Figure 18) was found at the Trapper (Duluth, MN) site. Movement below 300m occurs all day, but at 21:00 there are increases in density indicating the beginning of nocturnal migration. It is interesting that at 21:00, migrants are less dense than the same time period for Bad River. This may be due to migrants crossing over the end of Lake Superior, a journey of around 15 miles (25 km) delaying their arrival to this site. Migration densities and heights also decline after peaking around midnight, finally returning to daytime densities after the 04:00 hour.

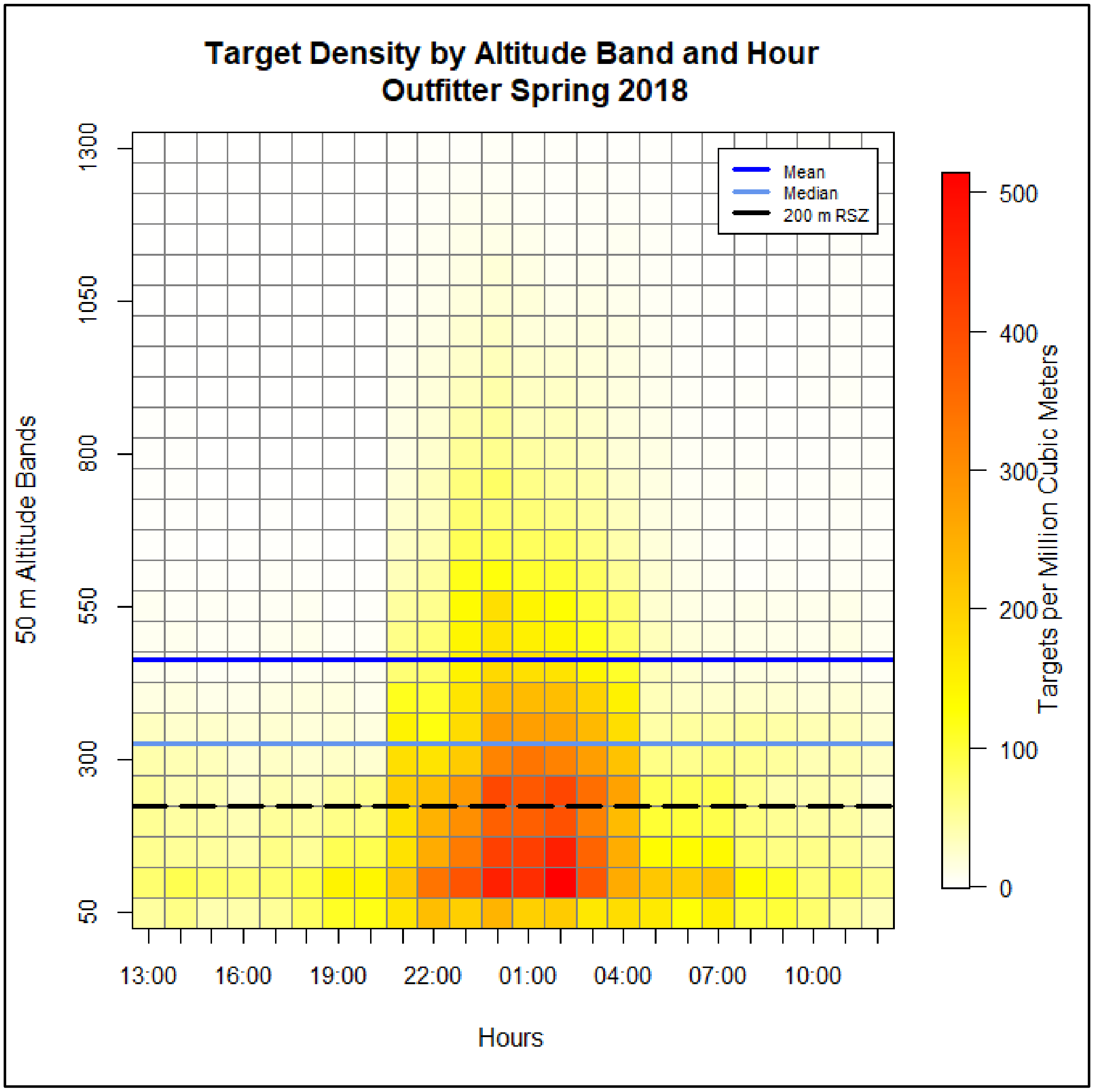

Figure 20. Hourly altitude heat map for Outfitter. The Y-axis depicts altitude in 50-meter bands, while the X-axis shows the hour, with midnight (0:00) as the midpoint of the axis. Cell colors depict density of migrants, corrected for radar beam shape, with warmer colors indicating higher target density. Uncorrected mean and median altitudes are depicted in dark and light blue lines, respectively. A 200 m rotor-swept zone is depicted by the dotted black line. The radar units sampled much higher than this 1300-m graph goes, but the bulk of the migrants moved in these lower altitudes, so ranges above 1300-m were not displayed.

On the North Shore of Lake Superior, the altitudinal pattern was quite different compared with the other two sites. On this shoreline, nocturnal migrants have mainly crossed over a large stretch of the open water to reach the site. The later time period of the highest density blocks is reflective of this: at the other sites, migration began at dusk, in the 21:00 hour, but at this site the heaviest migration did not occur until midnight. A crossing flight from Outer Island in the Apostle Islands to Grand Marais is about 45 miles (75 km) and the crossing from the base of the Keweenaw Peninsula is about 85 miles (135 km). These would take between 2-4 hours for migrants to cross, assuming a groundspeed of a passerine (25 mph; 12 m/s) (Bruderer and Bolt 2001). With most migrants setting out around 21:00 at the Bad River site, this estimated crossing time roughly matches with the arrival time at Grand Marais, MN. The altitudes observed at this site were also much lower than at the other sites. This could be due to a number of behaviors. First, migrants may be flying lower over the lake than over the land due to favorable wind conditions. Second, near the water surface, migrants may lower their altitude as they approach the shoreline in anticipation of landing to rest or to assess their location. Lastly, migrants may start out at a high altitude initially to find their navigational bearings and gradually lose altitude as they fly across the lake. Another unusual feature of this site is that migrants continue to arrive after dawn, especially at altitudes between 50-100 m, unlike the other locations. These likely represent migrants that were over the lake at dawn and had to finish their migration to the shoreline. These migrants likely land almost as soon as they reach the shoreline, both because they have been flying for much longer than they had planned, and because migrating during the light hours exposes them to predation. For this reason, the stopover habitat along the shoreline of this arriving shoreline may be very important to migrants, especially during the spring.

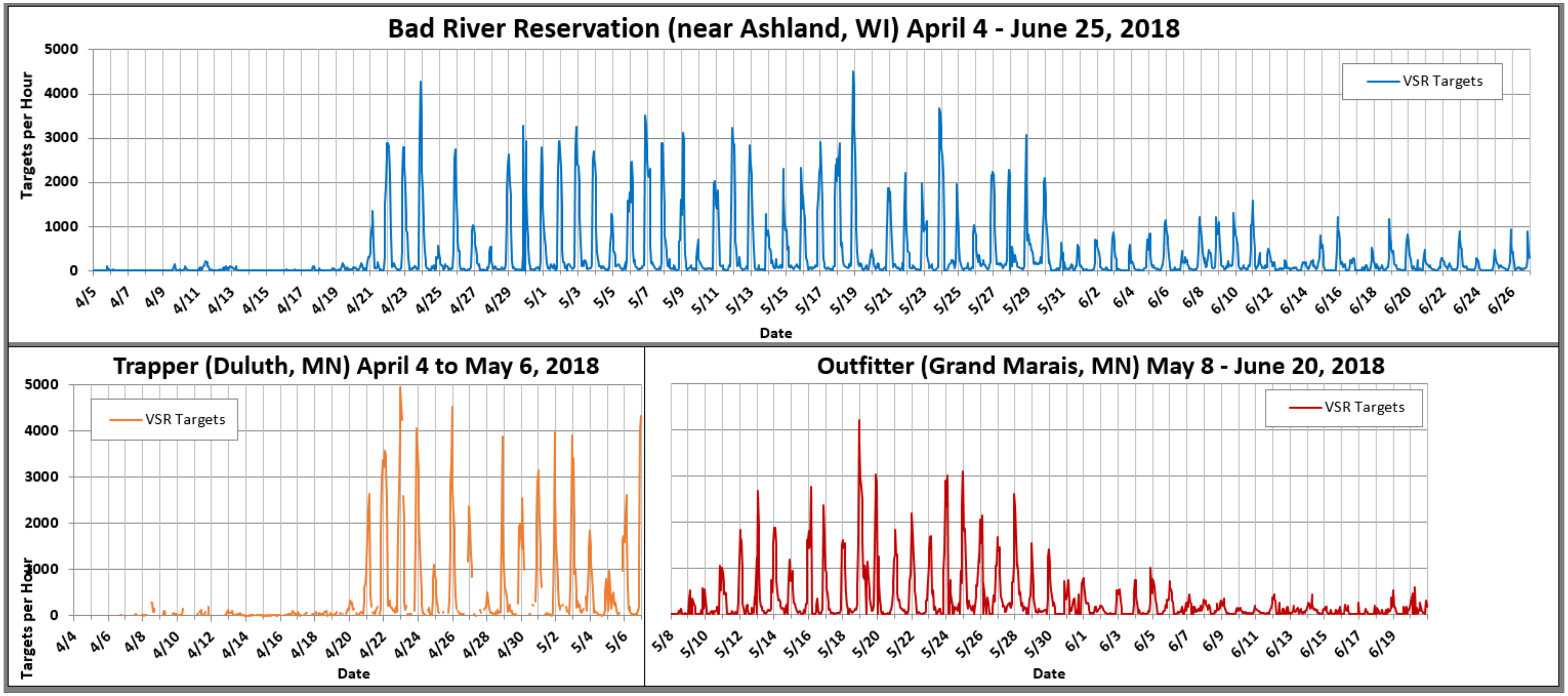

Figure 21. Timelines of each site for the Spring 2018 season aligned by date. Vertical (VSR) target counts are the only counts displayed. Starting and ending dates were different for each of the sites due to logistical factors of installing and removing the radar units. Total counts can be affected by a variety of factors, including clutter, that are unique to each site, so comparisons between sites in terms of numbers should be done with caution, however comparing the overall patterns between sites can be done.

Aligning the timelines from each of the sites across the season allows for pattern comparison among sites (Figure 21). Note that peaks of movement, onset of migration, and end of migration are very similar between each of the sites on Lake Superior substantial distances apart. This supports the assertion that larger environmental factors such as weather or storm fronts drive migratory movements. An example of this was for the early part of the season, these sites received an early April snowstorm that brought over a foot of snow. Once this snow melted (April 22), migrants started moving through the area. Migration moved through relatively consistently, and matched up peaks and valleys between each of the sites. The only notable difference between the sites was during the middle of the season, after shifting from Trapper to Outfitter sites. Migration was still occurring at Bad River, but at Outfitter, there was little movement. This may be that the migrants were delayed until early May due to the late snow and northern latitudes of the site, or simply that there was a local lull in migration that we happened to detect.

LITERATURE CITED

Akesson, S. 1999. Do passerine migrants captured at an inland site perform temporary reverse migration in autumn? Ardea 87:129-138.

Bruderer, B. 1997. The study of bird migration by radar, Part 1: The technical basis. Naturwissenschaften 84:1-8.

Bruderer, B., and A. Bolt. 2001. Flight characteristics of birds: I. radar measurements of speeds. Ibis 143:178–204.

Bruderer, B., and F. Liechti. 1998. Flight behaviour of nocturnally migrating birds in coastal areas: crossing or coasting. Journal of Avian Biology 29:499-507.

DeTect, Inc. 2009. MERLIN avian radar survey for a proposed wind project. Unpublished technical report. Panama City, FL.

Diehl, R.H., R.P. Larkin, and J.E. Black. 2003. Radar observations of bird migration over the Great Lakes. Auk 120:278-290.

Heist, K.W., T.S. Bowden, J. Ferguson, N.A. Rathbun, E.C. Olson, D.C. Nolfi, R. Horton, J.C. Gosse, D.H. Johnson, and M.T. Wells. 2018. Radar quantifies migrant concentration and Dawn reorientation at a Great Lakes shoreline. Movement Ecology 2018:6-15.

Kunz, T.H., E.B. Arnett, B.M. Cooper, W.P. Erickson, R.P. Larkin, T. Mabee, M.L. Morrison, M.D. Strickland, and J.M. Szewczak. 2007. Assessing impacts of wind-energy development on nocturnally active birds and bats: a guidance document. Journal of Wildlife Management 71:2449–2486.

Liechti, F., B. Bruderer, and H. Paproth. 1995. Quantification of nocturnal bird migration by moonwatching: comparison with radar and infrared observations. Journal of Field Ornithology 66:457–468.

Lowery, G.H. Jr. 1951. A quantitative study of the nocturnal migration of birds. University of Kansas Publications of the Museum of Natural History 3:361–472.

Myres, M.T. 1964. Dawn ascent and reorientation of Scandinavian thrushes (Turdus spp.) migrating at night over the northeastern Atlantic Ocean in autumn. Ibis 106:7–51.

Press, W.H., S.A. Teukolsky, W.T. Vetterling, and B.P. Flannery. 2007. *Numerical Recipes: The Art of Scientific Computing* (3rd ed.). New York: Cambridge University Press.

Rathbun, N.A., R.L. Horton, T.S. Bowden, E.C. Olson, D.C. Nolfi, D.J. Larson, and J.C. Gosse. 2016. Great Lakes Avian Radar Technical Report Delta County, MI Iosco County, MI, and Huron County, MI Fall 2012. U.S. Department of Interior, Fish and Wildlife Service, Biological Technical Publication FWS/BTPBTP-R3016-2017.(https://www.fws.gov/radar/documents/Avian%20Radar%20Fall%202012%20-Final%20October%202017%20HR.pdf)

Schmaljohann, H., F. Liechti, E. Baechler, T. Steuri, and B. Bruderer. 2008. Quantification of bird migration by radar - a detection probability problem. Ibis 150:342-355.

Zar, J.H. 1999. *Biostatistical Analysis* (4th ed.). Upper Saddle River, NJ: Prentice Hall.